Structural and Kinetic Description of Cytochrome *c* Unfolding Induced by the Interaction with Lipid Vesicles†

Teresa J. T. Pinheiro,*,‡,§ Gülnur A. Elöve,||,⊥ Anthony Watts,‡ and Heinrich Roder||

Institute for Cancer Research, Fox Chase Cancer Centre, 7701 Burholme Avenue, Philadelphia, Pennsylvania 19111, Department of Biochemistry, University of Oxford, South Parks Road, Oxford OX1 3QU, U.K., and Department of Biological Sciences, University of Warwick, Gibbet Hill Road, Coventry CV4 7AL, U.K.

Received May 27, 1997; Revised Manuscript Received August 4, 1997⊗

ABSTRACT: The interaction of cytochrome *c* with anionic lipid vesicles of DOPS induces an extensive disruption of the native structure of the protein. The kinetics of this lipid-induced unfolding process were investigated in a series of fluorescence- and absorbance-detected stopped-flow measurements. The results show that the tightly packed native structure of cytochrome *c* is disrupted at a rate of $\sim$1.5 s^{-1} (independent of protein and lipid concentration), leading to the formation of a lipid-inserted denatured state (D^L). Comparison with the expected rate of unfolding in solution ($\sim 2 \times 10^{-3}$ s^{-1} at pH 5.0 in the absence of denaturant) suggests that the lipid environment dramatically accelerates the structural unfolding process of cytochrome *c*. We propose that this acceleration is in part due to the low effective pH in the vicinity of the lipid headgroups. This hypothesis was tested by comparative kinetic measurements of acid unfolding of cytochrome *c* in solution. Our absorbance and fluorescence kinetic data, combined with a well-characterized mechanism for folding/unfolding of cytochrome *c* in solution, allow us to propose a kinetic mechanism for cytochrome *c* unfolding at the membrane surface. Binding of native cytochrome *c* in water (N^W) to DOPS vesicles is driven by the electrostatic interaction between positively charged residues in the protein and the negatively charged lipid headgroups on the membrane surface. This binding step occurs within the dead time of the stopped-flow experiments (<2 ms), where a membrane-associated native state (N^S) is formed. Unfolding of N^S driven by the acidic environment at the membrane surface is proposed to occur via a native-like intermediate lacking Met 80 ligation (M^S), as previously observed during unfolding in solution. The overall unfolding process ($N^S \rightarrow D^L$) is limited by the rate of disruption of the hydrophobic core in M^S. Equilibrium spectroscopic measurements by near-IR and Soret absorbance, fluorescence, and circular dichroism showed that D^L has native-like helical secondary structure, but shows no evidence for specific tertiary interactions. This lipid-denatured equilibrium state (D^L) is clearly more extensively unfolded than the A-state in solution, but is distinct from the unfolded protein in water (U^W), which has no stable secondary structure.

Structural and dynamic information on partially folded states of proteins has provided essential contributions toward understanding the mechanism of protein folding (Roder *et al.*, 1988; Radford *et al.*, 1992; Evans & Radford, 1994). In particular, the folding mechanism of cytochrome *c* (Elöve *et al.*, 1994) involves a complex interplay of various folding intermediates in multiple parallel folding pathways. An important feature of the folding process of this peripheral membrane protein is the ligation of a methionine at the sixth heme iron coordination site (Fe−Met 80). Detailed kinetic studies using a variety of conformational probes led to a comprehensive picture of the folding of cytochrome *c*. The fluorescence of a single tryptophan, Trp 59, which becomes quenched during folding through energy transfer with the heme (Tsong, 1976; Brems & Stellwagen, 1983), is a convenient parameter to monitor overall chain dimensions, and heme absorbance, which is a function of the oxidation, ligation, and spin states of the heme iron (Ikai *et al.*, 1973; Brems & Stellwagen, 1983), provides a sensitive measure of heme coordination during folding. The far-UV and near-UV regions of the circular dichroism (CD)[1] spectrum, which report on the secondary structure and burial of the aromatic side chains, respectively (Elöve *et al.*, 1992), and amide hydrogen exchange labeling combined with two-dimensional NMR methods (Roder *et al.*, 1988; Elöve & Roder, 1991) represent complementary probes for various structural features. Thus, four stages of the folding for cytochrome *c* have been identified (Elöve *et al.*, 1994), namely, a burst phase (<2 ms), in which a condensed state with fluctuating helical secondary structure is formed; a fast phase (2−100 ms), in which a partially folded intermediate with a native-like hydrophobic core involving extensive contacts between the

† This work has been supported by the EC Human Capital and Mobility Programme, Grant CT 920018 (A.W.); the Human Frontier Science Programme (T.J.T.P.); NIH Grants GM35926 and CAO6927 (H.R.); an appropriation from the Commonwealth of Pennsylvania; and The Royal Society. T.J.T.P. is a Royal Society University Research Fellow at Warwick.

* Correspondence should be addressed to this author at the University of Warwick. Telephone: +44 1203 528 364. Fax: +44 1203 523 568. E-mail: tp@dna.bio.warwick.ac.uk.

‡ Uniersity of Oxford.

§ University of Warwick.

|| Fox Chase Cancer Centre.

⊥ Present address: Regeneron Pharmaceuticals, Inc., 777 Old Saw Mill River Rd., Tarrytown, NY 10591-6707.

⊗ Abstract published in *Advance ACS Abstracts,* October 1, 1997.

[1] Abbreviations: CD, circular dichroism; DOPS, dioleoylphosphatidylserine; FTIR, Fourier transform infrared spectroscopy; GuHCl, guanidine hydrochloride; NMR, nuclear magnetic resonance.

S0006-2960(97)01235-X CCC: $14.00

N- and C-terminal α-helices is formed; an intermediate phase (100 ms to 1 s), where the native Met 80 ligation is formed after competition with other nonnative ligands; and a slow phase (>1 s), probably associated with proline isomerization (Ramdas & Nall, 1986).

Partially folded equilibrium states of cytochrome *c* have been described at acidic pH in the presence of salt (Ohgushi & Wada, 1983; Goto *et al.*, 1990; Jeng *et al.*, 1990; Jeng & Englander, 1991), and kinetic intermediates have been detected in refolding from urea- (Pryse *et al.*, 1992) or GuHCl-denatured protein (*e.g.*, Elöve *et al.*, 1994). Destabilization of the native structure of cytochrome *c* has also been reported in nondenaturing conditions during binding to anionic lipid membranes. Lipid-dependent conformational changes in membrane-bound cytochrome *c* were shown by resonance Raman spectroscopy (Heimburg *et al.*, 1991). This study demonstrated that conformational and coordination shifts are induced in lipid-bound cytochrome *c*, resulting in the opening of the heme crevice and formation of a five-coordinate high-spin iron state in equilibrium with the native six-coordinate low-spin form. Static and magic angle spinning phosphorus-31 NMR in various lipid−cytochrome *c* complexes (Spooner & Watts, 1991b, 1992; Pinheiro & Watts, 1994a,b) has provided additional evidence for the formation of a high−spin form of cytochrome *c* in lipid membranes. The lipid ^{31}P spin−lattice relaxation behavior is consistent with the disruption of Met 80 coordination and concomitant heme crevice opening, which allows close interaction of the heme with the lipid phosphate headgroup.

In addition to local perturbations within and around the heme crevice, an overall destabilization of the tertiary structure of cytochrome *c* bound to lipid membranes has been proposed. Solid-state ^{2}H NMR studies of cytochrome *c* bound to cardiolipin bilayers (Spooner & Watts, 1991a) and high-resolution ^{1}H NMR studies of cytochrome *c* bound to lipid-based detergent micelles (De Jongh *et al.*, 1992) have revealed extensive perturbation of the overall structure, as measured by enhanced exchange rates of amide deuterons in the lipid−protein complexes. Using FTIR spectroscopy, Heimburg and Marsh (1993) observed large changes in the amide proton exchange rates, as monitored by the spectral shifts in the amide I band of the protein in D_2O. In contrast, the amide I region of the FTIR difference spectrum between free and bound protein showed no appreciable temperature dependence at temperatures below that of denaturation. These results clearly show that upon binding to negatively charged lipid membranes, cytochrome *c* undergoes a substantial disruption of the tertiary structure with only small perturbations in secondary structure. Muga *et al.* (1991) previously arrived at a similar conclusion based on more qualitative results obtained by FTIR and differential scanning calorimetry.

It has been suggested that there is a close analogy between folding intermediates, in particular molten globule states, and the membrane-bound forms of soluble proteins (Bychkova & Ptitsyn, 1993). Such lipid-induced intermediates have been reported in the case of some bacterial toxins, such as colicin A (Van der Goot *et al.*, 1991) and colicin E1 (Lakey *et al.*, 1992). Studies on the interaction of cytochrome *c* with lipid membranes have suggested that a molten globule-like intermediate is formed during the interaction with model lipid membranes (De Jongh *et al.*, 1992; Spooner & Watts, 1992; Pinheiro & Watts, 1994a), but further structural and kinetic data are required to fully characterize this membrane-bound conformation. The availability of a well-characterized folding mechanism for cytochrome *c* in solution (Elöve *et al.*, 1994), and structural and kinetic folding intermediates involved therein (Roder *et al.*, 1988; Elöve & Roder, 1991), combined with well-described lipid−protein interactions, makes cytochrome *c* a good candidate to investigate protein folding events in the membrane environment.

Here we describe the structural changes in cytochrome *c* upon binding to vesicles formed by the anionic phospholipid DOPS. By monitoring the heme absorbance, Trp 59 fluorescence, and the CD spectral properties of cytochrome *c* in the lipid-bound form, we show that the native structure of cytochrome *c* is converted into a membrane-inserted denatured state, D^L, which has native-like secondary structure, but is expanded and lacks many features of the native tertiary structure, including tight packing of core residues and ligation of Met 80. The kinetics of lipid-induced unfolding of cytochrome *c* were studied by stopped-flow spectroscopic methods, monitoring Trp 59 fluorescence and Soret absorbance. It was found that the tightly packed native structure is disrupted at a rate of about 1.5 s^{-1}, which is orders of magnitude faster than the expected rate of unfolding in solution. Thus, the lipid environment dramatically accelerates the structural unfolding process of cytochrome *c*. We propose a mechanism for lipid-induced unfolding that explains this acceleration in terms of the localized acidic environment at the membrane surface. By analogy to the mechanism of folding and unfolding in solution, we propose that the unfolding of cytochrome *c* at the membrane surface follows a predominant pathway through a native-like intermediate lacking Met 80 ligation. The findings are discussed in the context of the well-characterized folding and unfolding mechanism of cytochrome *c* in solution, and have some general implications with respect to a possible mechanism for protein insertion and translocation across lipid membranes.

EXPERIMENTAL PROCEDURES

Materials. Cytochrome *c* from horse heart (type VI, Sigma Chemical Co.) was used without further purification. DOPS was purchased from Avanti Polar Lipids, Inc. (Birmingham, AL); and the tripeptide, Lys-Trp-Lys, was obtained from Sigma Chemical Co.

Sample Preparation. Aqueous solutions of cytochrome *c* were prepared in 10 mM phosphate buffer at pH 7.0. Protein concentrations were measured spectrophotometrically using a molar absorptivity of 2.95×10^4 M^{-1} cm^{-1} at 550 nm and pH 7.0 for the protein reduced with sodium dithionite (Margoliash & Walasek, 1967). For the preparation of DOPS vesicles, a dry film of 25 or 50 mg of lipid was produced under rotary evaporation from a stock solution in chloroform, which was then left under high vacuum for a minimum of 8 h to remove all traces of organic solvent. The lipid film was hydrated to the desired concentration with 10 mM phosphate buffer, pH 7.0. The buffer was deoxygenated with argon gas, and all steps of lipid hydration were carried out in an argon atmosphere. The resulting multilamellar liposome suspension was sonicated for several hours (in average about 3 h) in a bath sonicator (Solidstate Ultrasonic FS-14, Fisher Scientific), until a clear suspension of small unilamellar vesicles was obtained. The vesicle sizes of a

few representative samples were determined by dynamic light scattering measurements on a Dyna-Pro 801 dynamic light scattering instrument. Protein-free lipid vesicles had diameters ranging from 300 to 600 Å, and lipid−protein complexes showed a diameter range between 380 and 700 Å.

Absorbance Measurements. Absorbance spectra in the Soret (350−490 nm) and the 600−750 nm regions were obtained on samples containing 10−40 μM cytochrome *c* in 10 mM phosphate buffer, pH 7.0, in the presence or absence of DOPS vesicles. Typical concentrations of lipid varied from 2.5 to 10 mM in 10 mM phosphate buffer, pH 7.0. Spectra of the lipid−protein complexes were measured against a reference containing lipid vesicles in the same concentration as that in the measuring cell. All spectra were recorded at room temperature on a Perkin-Elmer Lambda 4B UV/VIS spectrophotometer.

Equilibrium Fluorescence and Manual-Mixing Kinetic Measurements. Equilibrium fluorescence spectra and manual-mixing kinetics were obtained on an AMINCO-Bowman Series 2 luminescence spectrometer (SLM-AMINCO, Urbana, IL), equipped with a water-jacketed cuvette holder and a circulating water bath. Sample temperature was controlled within an accuracy of ±0.2 °C. The excitation wavelength was 295 nm (2 nm band-pass), and emission spectra were recorded with a 4 nm band-pass. Cytochrome *c* concentrations, in 10 mM phosphate buffer, pH 7.0, varied from 5 to 20 μM, and DOPS from 2.5 to 10 mM. Time-dependent fluorescence changes over a time range from 20 to 900 s were monitored after rapid manual-mixing of equal volumes of preequilibrated solutions of protein and lipid vesicles at 20 °C. Tryptophan fluorescence was excited at 295 nm (band-pass of 2 nm), and kinetic traces were recorded at an emission wavelength of 330 nm (band-pass 4 nm).

Circular Dichroism. Circular dichroism spectra were measured in samples of 10 or 20 μM cytochrome *c* in 10 mM phosphate buffer, pH 7.0, in the presence or absence of lipid vesicles. Spectra were recorded at room temperature on a JASCO Model J720 spectropolarimeter. CD spectra of the far-UV (185−260 nm) and Soret regions were measured using quartz cells of 1 mm path length; for near-UV (250−350 nm) measurements, 10 mm path length cells were used. Typically, a scanning rate of 50 nm/min, a time constant of 1 s, and a band width of 1.0 nm were used. Spectral resolution was 0.5 or 1 nm, and 4−8 scans were averaged per spectrum. Spectra of lipid−protein complexes were subtracted from the background arising from the lipid vesicles alone.

Stopped-Flow Fluorescence Measurements. The kinetic fluorescence experiments were performed on a PQ/SF-53 stopped-flow instrument (Hi-Tech, Salisbury, U.K.) equipped with a Berger-type mixing chamber and a 2 × 2 × 10 mm flow cell. A 75 W xenon lamp (On-Line Instrument Systems, Inc., Jefferson, GA) and monochromator (Hi-Tech) were used for excitation at 295 nm (5 nm bandwidth) along the 10 mm axis of the cell. The fluorescence emission was detected in the 2 mm direction, using a high-pass glass filter with a 320 nm cutoff. The stopped-flow module and observation cell were thermostated with circulating water from a temperature-controlled water bath. All stopped-flow experiments were performed at 20 °C, and the sample temperature was measured to an accuracy of ±0.2 °C. Lipid-induced unfolding of cytochrome *c* was initiated by mixing equal volumes of cytochrome *c* in 10 mM phosphate buffer, pH 7.0, with DOPS vesicles in the same buffer (instrumental dead time 2.2 ms). Data acquisition and analysis have been described previously (Elöve *et al.*, 1992).

Absorbance-Detected Stopped-Flow Measurements. Unfolding kinetics of cytochrome *c* induced by interaction with lipid vesicles, and by pH-jump, were monitored by heme absorbance with a Biologic SFM4 stopped-flow instrument (Biologic, 38640 Claix, France) with a 2 mm flow cell. A tungsten lamp (LS-10, Hi-Tech) and monochromator were used to monitor the changes in Soret absorbance. For lipid-induced unfolding of cytochrome *c*, equal volumes of protein solution in 10 mM phosphate buffer, pH 7.0, and DOPS vesicles in the same buffer were rapidly mixed (dead time 2.4 ms). Acid-induced unfolding experiments were initiated by pH-jump experiments in which the initial solution of cytochrome *c* in H_2O, pH 5.0, was diluted 6-fold into 10 mM HCl solution, pH 2.0, in the absence or in the presence of 1.5 M NaCl. Kinetic data were collected and analyzed using software written in the ASYST programming language (Keithley Metrobyte). Data were acquired continuously at or near the maximum sampling time of 49 μs for 10−180 s kinetic traces and logarithmically averaged during acquisition to yield 85−110 data points. All measurements were carried at 20 °C, and for each experiment, four kinetic traces were averaged.

RESULTS

Met 80 Ligation. The axial coordination *via* the sulfur atom of Met 80 to the heme iron in cytochrome *c* results in a characteristic absorbance band at 695 nm; this S−Fe bond is intrinsically not very stable. Indeed, dissociation of the Met 80 coordination can readily occur under mild denaturing conditions, including pH values below 3 or above 9 (Greenwood & Palmer, 1965; Davis *et al.*, 1974; Dyson & Beattie, 1982), or by competitive binding of extrinsic ligands, such as cyanide or imidazole (Gao *et al.*, 1989). Disruption of the Met 80−iron bond as indicated by the loss of the 695 nm absorbance band has been interpreted as an opening of the heme crevice (Gao *et al.*, 1989). Soret absorbance (410 nm) mainly reports on changes in the spin state of the heme iron due to changes in its axial ligands (Brems & Stellwagen, 1983).

On binding of cytochrome *c* to DOPS vesicles, the 695 nm band disappears (Figure 1B), and the 410 nm band, characteristic of the native conformation of cytochrome *c* in aqueous solution, is shifted to 407 nm (Figure 1A). These changes are consistent with the disruption of Met 80 coordination to the heme iron upon binding the anionic lipid bilayers, as shown in previous studies (Heimburg *et al.*, 1991; Spooner & Watts, 1991a,b, 1992; Pinheiro & Watts, 1994a,b).

Equilibrium Fluorescence Changes. The fluorescence of a single tryptophan (Trp 59) in the polypeptide chain of cytochrome *c* was used to monitor the conformational changes in cytochrome *c* induced by its interaction with lipid. The fluorescence emission of Trp 59 in native cytochrome *c* in aqueous solution is completely quenched through Förster energy transfer with the heme (Figure 2). On binding to DOPS vesicles, there is a substantial increase in the fluorescence emission of cytochrome *c*, with an emission maximum around 330 nm (Figure 2). Urea-denatured cytochrome *c* shows an emission maximum near 345 nm (Figure 2). The binding of the tripeptide, Lys-Trp-Lys, to

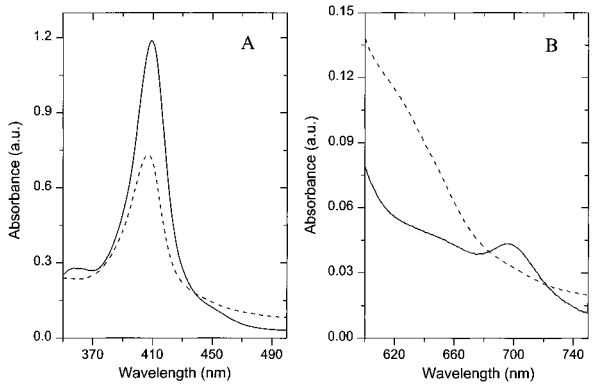

FIGURE 1: Absorbance spectra of cytochrome *c* in aqueous solution (solid line) and when bound to DOPS vesicles (dashed line). (A) Soret region (λ_{max} ~410 nm) and (B) near-IR region with the 695 nm absorbance band. Cytochrome *c* concentrations: 20 μM (A) and 40 μM (B); [DOPS], 5 mM. Spectra were obtained at room temperature (~21 °C), using cells with path lengths of 5 mm (A) and 1 cm (B).

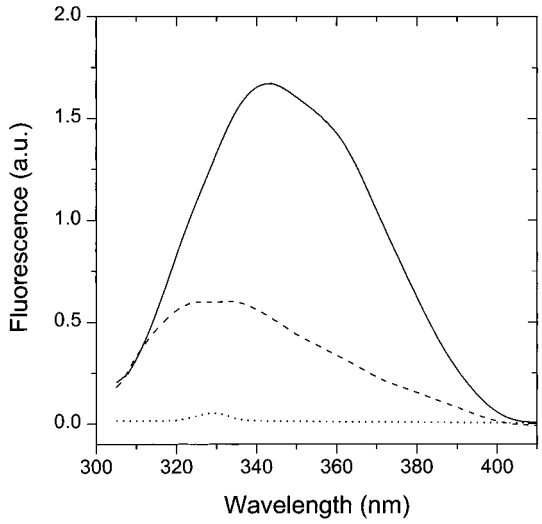

FIGURE 2: Equilibrium fluorescence emission spectra of native cytochrome *c* in aqueous solution (dotted line), cytochrome *c* bound to DOPS vesicles (dashed line), and urea-denatured cytochrome *c* in aqueous solution (solid line). Protein concentration, 20 μM; [DOPS], 5 mM; [urea], 10 M; temperature, 20 °C. The excitation wavelength was 295 nm.

DOPS vesicles shows a blue shift of about 14 nm (data not shown) when compared with the emission maximum in aqueous solution, and no significant changes in the overall fluorescence intensity are observed. Fluorescence emission spectra of lipid-bound cytochrome *c* after excitation at 295 nm, compared to the emission spectrum following excitation at 280 nm, demonstrate that an appreciable spectral contribution at lower wavelengths (300−330 nm) arises from some of the four tyrosines in the protein polypeptide chain. However, the blue shift and reduced spectral intensity of the fluorescence emission for membrane-bound cytochrome *c* relative to the urea-denatured form are indicative of a relatively more hydrophobic environment for Trp 59 when in lipid membranes, and show that some partial quenching through energy transfer with the heme is still present.

Secondary and Tertiary Structural Changes in Cytochrome c upon Interaction with Lipid Vesicles. Circular dichroism was used to monitor the effects of the interaction with lipid vesicles on the structural and conformational properties of

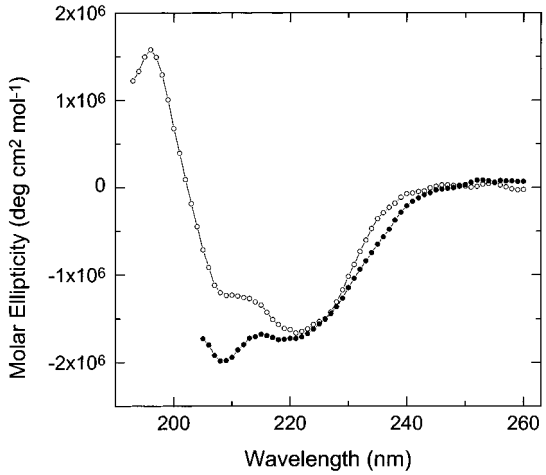

FIGURE 3: Far-UV CD spectra of cytochrome *c* in aqueous solution (open symbols) and when bound to DOPS vesicles (filled symbols). Protein concentration 10 μM; [DOPS], 5 mM. Spectra were recorded at room temperature (~22 °C), using a 1 mm path length cell at a resolution of 1 nm; 4 scans were averaged per spectrum.

cytochrome *c*. The far-UV CD spectrum of cytochrome *c* in solution (Figure 3) shows the typical features characteristic of proteins containing mainly α-helical structure (Chang *et al.*, 1978), in which the 222 nm dichroic band is predominantly associated with α-helical $n-\pi^*$ amide transitions, and the negative minimum at around 209 nm and the positive maximum about 190 nm are the dichroic bands corresponding to the $\pi-\pi^*$ amide transitions (Myer, 1968b). Upon binding to DOPS vesicles, no substantial change is observed in the far-UV CD band at 222 nm (Figure 3), suggesting that there are no significant changes in the α-helix content. The spectral changes around the minimum at 209 nm may arise from changes in other secondary structure elements in the protein, or may be due to the presence of optically active heme transitions other than those associated with the amide transitions of the polypeptide chain. Therefore, an unambiguous interpretation of the spectral changes on this region of the spectrum is not possible.

Near-UV (250−330 nm) circular dichroism is a probe for protein tertiary structure changes that affect the environment of aromatic side chains. Horse cytochrome *c* contains four phenylalanine residues, four tyrosine residues, one tryptophan, and two thioether bonds, all of which can potentially contribute to the near-UV CD spectrum. Unfortunately, the interpretation of this region of the CD spectrum is further complicated by the optically active heme transitions that occur between 240 and 300 nm (Urry, 1967). Tyrosine residues produce CD vibronic transition bands with maxima between 275 and 282 nm, while phenylalanine side chains can produce weak CD bands between 255 and 270 nm (Strickland, 1974). A broad positive CD band around 263 nm has been attributed to porphyrin transitions with rotary strengths dependent on the immediate environment of the heme group (Urry, 1967). The sharp minima in the CD spectrum of cytochrome *c* at 282 and 288 nm (Figure 4) are assigned to the Trp 59 side chain, as confirmed by site-directed mutagenesis (Davies *et al.*, 1993). On binding to DOPS vesicles, these near-UV CD spectral markers of the tertiary structure disappeared (Figure 4), which is consistent with a disruption of the tight packing of core residues in cytochrome *c* upon interaction with the lipid vesicles. Indeed, the near-UV CD spectrum of lipid-bound cytochrome

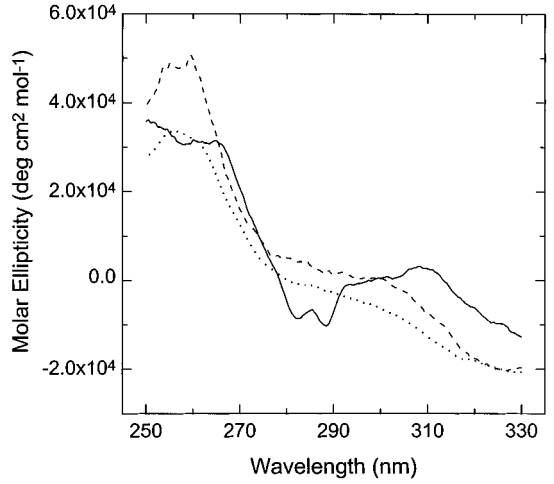

FIGURE 4: Near-UV CD spectra of cytochrome *c* in aqueous solution (solid line), bound to DOPS vesicles (dashed line), and denatured in 4.2 M GuHCl (dotted line). Protein concentration, 20 μM; [DOPS], 5 mM. Spectra were recorded at room temperature (~22 °C), using a 10 mm path length cell at a resolution of 0.5 nm; 8 scans were averaged per spectrum.

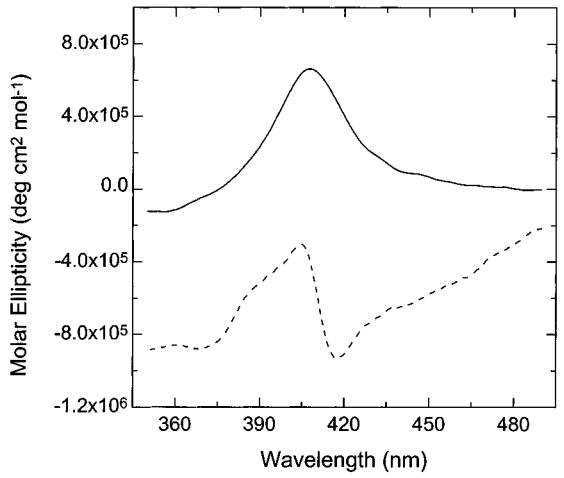

FIGURE 5: CD spectra of the Soret region of cytochrome *c* in aqueous solution (dashed line) and bound to DOPS vesicles (solid line). Protein concentration, 20 μM; [DOPS], 5 mM. Spectra were obtained at room temperature (~22 °C), using a 10 mm path length cell; 0.5 nm resolution; 4 scans were averaged per spectrum.

c resembles that of GuHCl-denatured cytochrome *c*, as shown in Figure 4.

The CD spectrum in the Soret region can provide further insight into the integrity of the heme crevice (Myer, 1968b). The optical activity in the Soret region of heme proteins is generated through the coupling of heme $\pi-\pi^*$ electric dipole transition moments with those of nearby aromatic amino acid residues in the protein (Hsu & Woody, 1971). The CD spectrum for cytochrome *c* in its native conformation shows a strong negative limb due to the Soret−Cotton effect (Figure 5), primarily as a result of heme−polypeptide interactions. After binding to the lipid membrane, the Soret CD spectrum changes to a single positive band with a maximum near 408 nm. This type of spectrum is also observed with urea-denatured cytochrome *c*, is induced by elevated temperature, extrinsic ligands, or pH-induced denaturation (Myer, 1968a), and was also reported for carboxymethylated cytochrome *c* (Santucci *et al.*, 1987, 1989). The observed changes in the Soret region clearly indicate a disruption of the coupling between $\pi-\pi^*$ transitions of the heme group and those of the aromatic amino acid residues in its proximity. This effect is consistent with a loosening of the tertiary structure, which removes the anisotropic character of the Soret circular dichroism band.

Fluorescence-Detected Unfolding Kinetics of Cytochrome c at the Membrane Surface. The fluorescence intensity changes of Trp 59 have been used to monitor the folding kinetics of cytochrome *c* in solution (Elöve *et al.*, 1992, 1994; Colón *et al.*, 1996). These studies normally start with an unfolded protein solution in a denaturing buffer, such as 4.5 M GuHCl, and folding is initiated by dilution of the denaturing agent. Upon folding, the fluorescence decays due to Förster energy transfer between the Trp 59 and the heme group. In the present study, kinetic measurements start with cytochrome *c* in its native conformation in aqueous buffer solution, in which the intrinsic fluorescence is largely quenched (see for example, Figure 2), and unfolding of cytochrome *c* induced by the interaction with lipid vesicles is monitored by the increase of tryptophan fluorescence in stopped-flow experiments. The changes in fluorescence emission (detected above 310 nm) relative to the native cytochrome *c* in buffer solution, and in the absence of lipid, are recorded over a time range up to 90 s after rapid mixing with the lipid vesicles. The fluorescence-detected stopped-flow unfolding kinetics of cytochrome *c* were monitored for various lipid and protein concentrations. Representative kinetic traces are shown in Figure 6A,B, where the increase in fluorescence is plotted on a logarithmic time scale. Stopped-flow control experiments in which DOPS vesicles were mixed with buffer in the absence of protein revealed a significant and somewhat variable scattering background, which was subracted from each kinetic trace. However, the scattering background remained constant over the measured time period, and the observed kinetic signal appears to be a reliable measure of the tryptophan fluorescence changes. Kinetic parameters were obtained by nonlinear least-squares fitting of a minimum number of exponential phases. A summary of rates and amplitudes is presented in Tables 1 and 2. For concentrations of cytochrome *c* above 15 μM, the kinetics are poorly represented by only two exponentials, and three exponential phases were used instead (see, for example, the double- and triple-exponential fitting for 15 μM cytochrome *c*, 10 mM DOPS, in Figures 6A,B, respectively). The kinetic parameters obtained by the two fitting procedures are included in Tables 1 and 2. We have also monitored the fluorescence changes at 330 nm (bandwidth 4 nm) in manual-mixing experiments over a time range of 900 s after a dead time of 20 s (data not shown), which revealed a biphasic increase in fluorescence with an additional slow phase not covered by the stopped-flow measurements. The corresponding rates and amplitudes are listed in Table 3.

The dependence of the total kinetic fluorescence amplitude as a function of cytochrome *c* concentration is shown in Figure 6C. Qualitatively, the intial increase in amplitude up to 15 μM cytochrome *c* can be interpreted as a 1:1 binding equilibrium with an apparent dissociation constant in the micromolar range. However, the analysis is complicated by the fact that the true vesicle concentration is not known (the "fit" in Figure 6C suggests a value of about 12 μM). Moreover, the marked decrease in amplitude above 15 μM cytochrome *c* suggests that the assumption of 1:1 stoichiometry is no longer valid at higher protein concentrations; binding of multiple cytochrome *c* molecules to the same

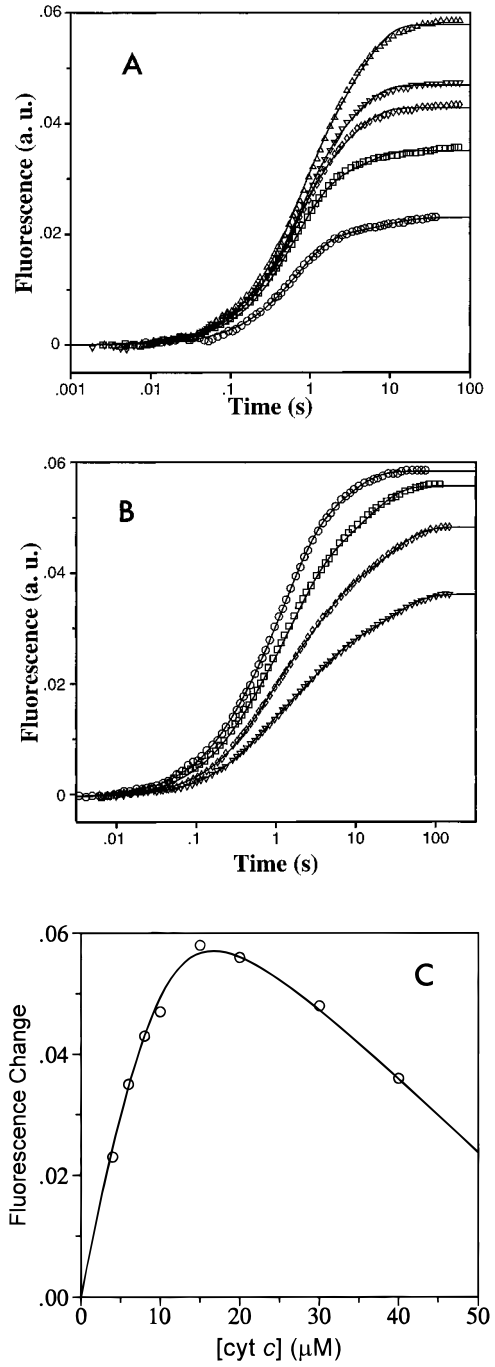

FIGURE 6: Representative fluorescence-detected unfolding kinetics of cytochrome *c* induced by binding to DOPS vesicles at 20 °C (10 mM phosphate buffer at pH 7.0). The fluorescence of tryptophan 59 (excited at 295 nm and detected above 310 nm) was measured in stopped-flow experiments (dead time ~2 ms), after mixing equal volumes of protein in aqueous solution with DOPS vesicles. The fluorescence change is plotted on a logarithmic time scale. Final DOPS concentration, 10 mM. (A) Final concentrations of cytochrome *c* were 4 μM (circles), 6 μM (squares), 8 μM (diamonds), 10 μM (downward triangles), and 15 μM (upward triangles). The curves are double-exponential least-squares fits (cf. Table 1). (B) Final concentrations of cytochrome *c* were 15 μM (circles), 20 μM (squares), 30 μM (diamonds), and 40 μM (downward triangles). The curves are triple-exponential least-squares fits (cf. Table 2). (C) Total kinetic amplitude (final base line values of kinetic traces in Figures 6A,B) as a function of cytochrome *c* concentration. The curve is for guidance only and has no clear theoretical significance (it represents a binding curve with a sloping base line, based on a 1:1 binding equilibrium with an apparent dissociation constant of about 1 μM and a vesicle concentration of 12 μM; see text).

Table 1: Fluorescence Kinetic Rates and Relative Amplitudes for Cytochrome *c* Partial Unfolding Induced by DOPS at Various Protein and Lipid Concentrations[a]

[DOPS] (mM)	[cyt *c*] (μM)	k_1 (s^{-1})	a_1 (%)[b]	k_2 (s^{-1})	a_2 (%)[b]	$-(a_1 + a_2)$[c]
10	2	1.37 (7)[d]	85.7	0.15 (7)	11.9	0.021
10	4	1.52 (4)	82.6	0.12 (2)	16.5	0.023
10	6	1.67 (4)	77.1	0.25 (2)	22.3	0.035
10	8	1.79 (8)	62.8	0.35 (3)	37.2	0.043
10	10	1.60 (6)	61.7	0.33 (2)	38.3	0.047
10	15	1.65 (7)	53.4	0.27 (1)	46.6	0.058
10	20	1.32 (5)	57.1	0.12 (1)	42.9	0.056
10	30	1.14 (4)	57.4	0.073 (4)	42.5	0.047
10	40	1.12 (4)	55.6	0.066 (4)	44.4	0.036
2.5	5	1.94 (7)	57.1	0.26 (1)	42.9	0.035
2.5	10	1.37 (5)	58.8	0.16 (1)	41.2	0.068
2.5	20[e]	3.2 (2)	39.3	0.44 (2)	60.7	0.061
1	2.5	1.83 (6)	56.6	0.28 (1)	43.4	0.106
1	5	1.09 (2)	64.1	0.19 (1)	35.9	0.170
1	10	1.08 (1)	53.1	0.098 (1)	46.9	0.294

[a] Rates and relative amplitudes were measured by stopped-flow fluorescence emission kinetic measurements at 20 °C, as described under Experimental Procedures. [b] Percentage of the total amplitude. [c] Total kinetic amplitude in arbitrary (but constant) fluorescence units. [d] Errors in the least significant digit (one standard deviation) are shown in parentheses. [e] At this protein concentration, data are best fitted with three exponentials (see Figure 6A,B), and the third phase has kinetic parameters $k_3 = 0.026$ (0.001) s^{-1}, $-(a_1 + a_2 + a_3) = 0.084$, and $a_3 = 27.4\%$.

vesicle may result in mutual fluorescence quenching. Complications due to protein−protein interaction in the lipid-bound state are also consistent with the kinetic data at cytochrome *c* concentrations of 15 μM and above (Figure 6B), which show an additional concentration-dependent phase not observed at lower concentrations.

The combined stopped-flow and manual-mixing data show evidence of four distinct kinetic events: (A) The initial second-order protein−vesicle binding step is expected to occur within the dead time (<2 ms). If association is diffusion-controlled, this second-order rate constant is expected to be of the order of 1×10^9 s^{-1}, which corresponds to a rate of about 5000 s^{-1} at 5 μM cytochrome *c*. Favorable electrostatic interactions could accelerate this process further. It is unlikely that this event is accompanied by any significant fluorescence changes because of the efficient quenching of Trp 59 fluorescence in native-like states and compact intermediates (Elöve *et al.*, 1992, 1994). (B) A major fluorescence increase (>80% of the observable change) occurs with a rate of ~1.5 s^{-1} (at cytochrome *c* concentrations <10 μM, and independent of DOPS concentration). (C) A minor process exists with a protein concentration-dependent rate (~0.1 s^{-1}) and amplitude (12% at 2 μM cyt *c*, ~50% above 15 μM cyt *c*), probably due to protein−protein interaction. (D) A slow fluorescence increase is seen only in manual-mixing experiments with a minor amplitude (~20% of total signal) and a rate ~0.01 s^{-1}, independent of DOPS concentration. Since only extensively unfolded states are strongly fluorescent, the phase with the largest fluorescence increase, process B, is likely to correspond to the main unfolding event associated with insertion into the lipid membrane. It is relevant to compare the rate of this main kinetic phase (1.5 s^{-1}) with that observed for the unfolding of cytochrome *c* in the absence of lipids. Linear extrapolation of the GuHCl-induced unfolding rate at pH 7 (Colón *et al.*, 1996) to 0 M GuHCl gives a rate of about 5×10^{-6} s^{-1}. At pH 5, this rate is faster, about 2×10^{-3} s^{-1} [unpublished;

Table 2: Fluorescence Kinetic Rates and Relative Amplitudes of Cytochrome *c* Partial Unfolding Induced by DOPS at Various Protein Concentrations[a]

[DOPS] (mM)	[cyt *c*] (μM)	k_1 (s^{-1})	a_1 (%)[b]	k_2 (s^{-1})	a_2 (%)[b]	k_3 (s^{-1})	a_3 (%)[b]	$-(a_1 + a_2 + a_3)$
10	15	4.8 (0.4)[c]	14.2	0.83 (0.03)	61.7	0.14 (0.01)	23.3	0.060
10	20	3.6 (0.3)	19.3	0.64 (0.03)	52.6	0.073 (0.003)	28.1	0.057
10	30	1.93 (0.08)	34.0	0.35 (0.02)	38.0	0.038 (0.002)	28.0	0.050
10	40	2.13 (0.08)	29.7	0.35 (0.02)	40.5	0.036 (0.001)	29.7	0.037

[a] Rates and relative amplitudes were measured by stopped-flow fluorescence emission kinetic measurements at 20 °C, as described under Experimental Procedures. [b] Percentage of the total amplitude. [c] Errors (one standard deviation) are shown in parentheses.

Table 3: Fluorescence Kinetic Rates and Relative Amplitudes for Cytochrome *c* Partial Unfolding at Various DOPS Concentrations[a]

[DOPS] (mM)	[cyt *c*] (μM)	$\lvert k_1$ (s^{-1})	a_1 (%)[b]	k_2 (s^{-1})	a_2 (%)[b]	$-(a_1 + a_2)$
1	10	6.4×10^{-2} (0.005)[c]	51.4	9.0×10^{-3} (0.0001)	48.6	0.35
0.5	10	4.1×10^{-2} (0.003)	47.8	5.8×10^{-3} (0.0001)	52.2	0.23
0.25	10	5.2×10^{-2} (0.002)	27.6	13.0×10^{-3} (0.0007)	72.4	0.076

[a] Rates and relative amplitudes were measured by manual-mixing fluorescence emision kinetic measurements at 20 °C, as shown in Figure 7 and described under Experimental Procedures. [b] Percentage of the total amplitude. [c] Errors (one standard deviation) are shown in parentheses.

see also Sosnick *et al.* (1996)], but still about 3 orders of magnitude slower than the DOPS-induced unfolding rate. This comparison rules out a mechanism in which the protein unfolds in solution before associating with lipid. Instead, it suggests that the lipid environment dramatically accelerates the structural unfolding process.

Absorbance-Detected Unfolding Kinetics. A possible mechanism for the lipid-induced cytochrome *c* unfolding may involve a localized acidic pH effect at the membrane surface (see below). In order to test this hypothesis, we have investigated the heme absorbance changes during cytochrome *c* unfolding induced by the interaction with lipid vesicles, and compare the rate of this process with that of acid-induced unfolding in solution. On binding to DOPS vesicles, we have observed a small shift of the Soret absorbance band from 410 nm in the native protein in solution to 407 nm in the lipid-bound form, in addition to a significant reduction of its intensity (Figure 1A). The heme absorption difference spectrum between native cytochrome *c* in solution and the lipid-bound state shows a pronounced maximum at 409 nm. We have measured the time-dependent spectral changes at 409 nm, 20 °C, in stopped-flow kinetic experiments (dead time 2.4 ms) following rapid mixing of cytochrome *c* in buffer solution (pH 7.0) with DOPS vesicles (pH 7.0). A main kinetic phase with a rate constant of about 0.7 s^{-1} was observed, independent of lipid or protein concentrations (Figure 7 and Table 4). This unfolding rate was compared with the acid-induced unfolding of cytochrome *c* in a pH jump experiment from 5 to 2, at 20 °C. At pH 5, cytochrome *c* shows the typical native Soret absorbance band at 410 nm. At pH 2, and in the absence of salt, cytochrome *c* is unfolded and its Soret band is shifted to 394 nm (data not shown). The difference absorption spectrum between pH 5.0 and pH 2.0 solutions of cytochrome *c* shows a pronounced maximum at 412 nm, and a minimum at 393 nm. A pH jump from 5 to 2, in the absence of salt, induces the transition from the native state (N) to the unfolded state (U) of cytochrome *c*, whereas in the presence of salt the transition from the N- to the A-state is observed instead (Dyson & Beattie, 1982; Goto *et al.*, 1990; Jeng *et al.*, 1990; Colón & Roder, 1996). Stopped-flow kinetic measurements of the spectral changes at 412 nm, following a rapid jump from pH 5.0 to pH 2.0, in the absence of salt, revealed a single kinetic phase (data not show) with a rate constant of 3.5 s^{-1} (Table 4). This rate is within a factor of 5 of the main lipid-induced unfolding phase detected by absorbance (0.7 s^{-1}), and within a factor of 2.5 of the main unfolding event observed by fluorescence-detected stopped-flow measurements (1.5 s^{-1}). Thus, compared to the over 1000-fold lower rate of unfolding at pH 5 and above, the rate of unfolding induced by the lipid matches that of the acid-induced process remarkably well.

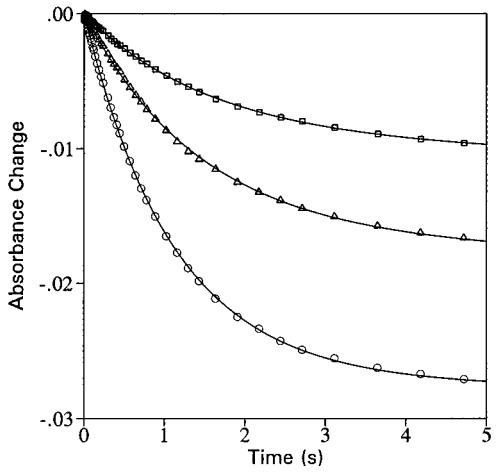

FIGURE 7: Unfolding kinetics of cytochrome *c* detected by heme absorbance upon binding to DOPS vesicles at 20 °C (10 mM phosphate buffer at pH 7.0). The Soret absorbance change at 409 nm was measured in stopped-flow experiments (dead time 2.4 ms), after mixing protein in buffer solution with DOPS vesicles. Final DOPS concentration, 2.5 mM; final concentrations of cytochrome *c* were 1.25 μM (squares), 2.5 μM (triangles), and 5 μM (circles). The curves are single-exponential least-squares fits.

DISCUSSION

Protein Unfolding on Membrane Surfaces. The interaction of water-soluble proteins with a membrane surface is a common process during the course of various cellular functions. Some examples include bacterial toxins (Parker & Pattus, 1993), precursor proteins that have to translocate across intracellular membranes in order to reach their final location in a particular cellular organelle (Hannavy *et al.*, 1993), and the class of proteins involved in the transfer of various nonpolar ligands, such as retinol and fatty acids, to

Table 4: Soret Absorbance Kinetic Rates and Relative Amplitudes of Cytochrome *c* Unfolding Induced by the Interaction with DOPS Vesicles and Comparison with Unfolding by pH Jump in Solution[a]

[DOPS] (mM)	[cyt *c*] (μM)	k_1 (s^{-1})	a_1 (ODU)
10	4	0.631 (9)[b]	0.031
10	8	0.713 (6)	0.056
10	12	0.707 (6)	0.078
2.5	1.25	0.661 (10)	0.009
2.5	2.5	0.704 (9)	0.016
2.5	5	0.908 (2)	0.027
pH jump[c]	12	3.53 (4)	0.102

[a] Rates and relative amplitudes obtained from kinetic measurements (20 °C) by stopped-flow Soret absorbance at 409 nm for lipid-induced unfolding, and at 414 nm for unfolding in solution induced by pH jump (5 → 2), as described under Experimental Procedures. [b] Errors in the least significant digit (one standard deviation) are shown in parentheses. [c] Unfolding kinetics were induced by 6-fold dilution of cytochrome *c* in water, pH 5, into 10 mM HCl, pH 2.0, in the absence of salt.

a target cell surface (Cowan *et al.*, 1990). The mechanism by which a water-soluble protein becomes associated with a membrane surface is at present poorly understood. However, it is becoming apparent that the transition from the water-soluble to the membrane-associated state involves major changes in the protein structure (Parker & Pattus, 1993; Banuelos & Muga, 1995, 1996). The nature of the structural intermediates involved in this transition is of general interest to the problem of protein folding. There are some indications that the interaction of a soluble protein with lipid membranes may occur through the molten globule state (Van der Goot, 1992; Banuelos & Muga, 1995), which is implicated in the folding mechanism of many proteins in solution (Ptitsyn, 1995).

The existence of well-characterized intermediates in the folding mechanism of cytochrome *c* in solution under a variety of refolding conditions makes this protein an excellent model to investigate the mechanism of protein interaction with a membrane surface and the intricate relationship with protein folding events. In contrast to refolding experiments of cytochrome *c* in solution in which folding to the native state is achieved by dilution of a denaturant [see, for example, Elöve *et al.* (1992, 1994) and Colón *et al.* (1996)], we consider here the reverse process of unfolding of cytochrome *c* from its fully folded state in solution to a partially unfolded membrane-bound state. Our circular dichroism results show that upon binding to negatively charged lipid vesicles several features of the tertiary structure of cytochrome *c* change with no significant perturbation of the overall secondary structure (Figures 3 and 4). The Soret CD spectrum (Figure 5) shows a highly perturbed heme crevice, resembling that obtained under denaturing conditions, for example, in the presence of urea or extrinsic ligands, at elevated temperatures, or at extreme pH (Myer, 1968a).

The intrinsic protein fluorescence, mainly from a single tryptophan at position 59 with a minor contribution from some of the four tyrosines in cytochrome *c*, is a very sensitive probe for monitoring the overall conformation of cytochrome *c*. Whereas the fluorescence of Trp 59 in the compact native state is completely quenched due to its close proximity to the heme group (Figure 2), unfolding of cytochrome *c* induced by binding to DOPS vesicles is accompanied by a substantial increase in fluorescence (Figure 2). The fluorescence quantum yield of lipid-bound cytochrome *c* is about 32.5% of the fully unfolded protein in urea, and the emission maximum has a significant blue shift of about 15 nm relative to the emission maximum of urea-denatured protein (Figure 2). The binding of a short model peptide, Lys-Trp-Lys, to the same lipid vesicles showed a comparable blue shift, but no significant change in the fluorescence quantum yield. This clearly indicates that the observed increase in Trp 59 fluorescence in the lipid environment is the result of protein conformational changes, described here as lipid-induced unfolding. The blue shift for the emission maximum of lipid-bound cytochrome *c* relative to the urea-denatured state is consistent with the effect observed by changing the Trp environment from an aqueous solution to the lipid hydrophobic phase, as observed for Lys-Trp-Lys.

Cytochrome c Unfolding and Met 80 Deligation. Unfolding studies of cytochrome *c* at high GuHCl concentrations have revealed a nearly denaturant-independent kinetic process associated with formation of a native-like intermediate lacking Met 80 ligation (Colón *et al.*, 1996). This interpretation is consistent with the fact that the Met 80 ligand can be displaced by addition of extrinsic ligands, such as imidazole, cyanide, or azide, resulting in a folded state with native-like structural properties (Babul & Stellwagen, 1971; Roder *et al.*, 1986), and has been recently confirmed by kinetic measurements in which Met 80 ligation is displaced by imidazole (Colón and Roder, in preparation). It was found that at lower denaturant concentrations the rate of the main structural unfolding event is the rate-limiting step. This rate increases with GuHCl concentration and eventually becomes faster than the rate of Met 80 dissociation (GuHCl concentrations above 4 M), so that deligation of Met 80 becomes the rate-limiting step. This strongly suggests that unfolding of cytochrome *c* requires the Met 80 ligand to be dissociated before the main structural unfolding process can proceed. This has indeed been demonstrated in a study on a homologous bacterial protein, cytochrome c_2 (Sauder *et al.*, 1996), in which the deligation kinetics of Met 96 (equivalent to Met 80 in horse cytochrome *c*) were investigated by imidazole binding experiments.

In our present work, the absence of the absorbance band at 695 nm (Figure 1B) shows that Met 80 is not ligated to the heme iron in the lipid-bound conformation. The susceptibility of this coordination to high ionic strength (Gao *et al.*, 1989) suggests that the electrostatic interaction with the charged membrane surface may induce the disruption of Met 80−iron ligation, facilitating the subsequent structural unfolding of cytochrome *c*. A possible mechanism of how a negatively charged membrane surface can promote protein unfolding requires the consideration of local pH. The high density of negatively charged groups on the membrane surface creates a strong electrostatic potential which attracts protons, thus leading to a substantial decrease of the local pH at the membrane surface. It has been shown that this decrease in pH can be as large as 1.8 pH units at 5−15 Å from the membrane interface plane, and as much as 4.2 pH units in the immediate vicinity of the membrane surface (Prats *et al.*, 1986). It is also well-known that moderately low pH can lead to formation of partially unfolded molten globule states for many proteins (for a review, see Ptitsyn (1995)].

We observed by fluorescence a main kinetic phase for lipid-induced unfolding of cytochrome *c* with a rate of about 1.5 s^{-1} and 80% of the total observed amplitude at low

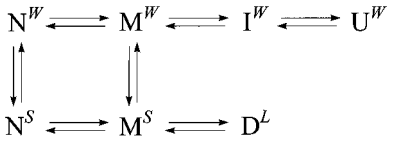

FIGURE 8: Scheme of the proposed kinetic unfolding mechanism of cytochrome *c* induced by the interaction with negatively charged lipid membranes. N represents the folded native conformation in water (N^W) or associated with the membrane surface (N^S); M is a native-like intermediate lacking Met 80 ligation in water (M^W) or associated with the membrane surface (M^S). I^W denotes a compact intermediate state in water. U^W designates the unfolded state in solution, and D^L represents a denatured state inserted into the lipid membrane. Unlike U^W, which has no stable secondary structure, D^L has native-like helical secondary structure, but is at least partially unfolded in terms of several features of its tertiary structure (*see* Results and Discussion sections). Unfolding of cytochrome *c* induced upon binding to DOPS vesicles follows a predominant pathway through N^S and M^S. Binding of cytochrome *c* to the membrane surface ($N^W \rightarrow N^S$) occurs rapidly (<ms), and the compact native-like intermediate N^S is disrupted at rate of ~1.5 s^{-1}.

protein concentrations (Table 1). A comparison of this rate with that observed for GuHCl-induced unfolding extrapolated to zero denaturant concentration (5×10^{-6} s^{-1} at pH 7, and 2×10^{-3} s^{-1} at pH 5; Colón *et al.*, 1996; Sosnick *et al.*, 1996) suggests that the lipid environment strongly accelerates the main structural unfolding process. The recent studies by Colón *et al.* (1996) and Sauder *et al.* (1996) have shown that unfolding of cytochrome *c* in solution from its native sate (N^W, see Figure 8) occurs preferably via an obligatory intermediate lacking Met 80 ligation (M^W). Deligation of Met 80 precedes the main structural unfolding and is the rate-limiting step under strongly denaturing conditions (Colón *et al.*, 1996; Sauder *et al.*, 1996). In this regime, the rate of the main structural unfolding transition is faster than Met 80 deligation. The Soret absorbance-detected kinetics of the lipid-induced unfolding of cytochrome *c* revealed a single kinetic process with a rate of 0.7 s^{-1}, which is consistent with the main unfolding event in the fluorescence-detected kinetics (~1.5 s^{-1}). This is further supported by comparison with the rate of acid-induced unfolding of cytochrome *c* in the absence of salt monitored by Soret absorbance (N to U transition), which showed a main kinetic process with a rate of 3.5 s^{-1} (Table 4). In similar experiments carried out in the presence of salt (N- to A-state transition), 97% of the total observed absorbance change is lost in the dead time of this experiment (2.4 ms), indicating that formation of the A-state (which probably includes deligation of Met 80) escapes our detection. Thus, methionine deligation appears to be a very rapid (less than milliseconds) process at low pH, and the observed kinetics of the N to U transition appear to reflect the main structural unfolding step of cytochrome *c*. Previous unfolding studies on cytochrome *c* revealed that the limiting rate of unfolding, associated with deligation of Met 80, is dependent on pH and the presence of salt in high denaturant concentrations. This rate increases toward lower pH and higher salt concentration: 50 s^{-1} at pH 7.0 (Colón *et al.*, 1996), ~80 s^{-1} at pH 5.0 (Colón *et al.*, unpublished results), and ~120 s^{-1} at pH 4.9 and higher salt concentration (Sosnick *et al.*, 1996), all at 10 °C. Two interesting observations can be made by comparing these rates with the observed rate of lipid-induced unfolding (1.5 s^{-1}). First, the trend of variation with pH for the limiting rate of unfolding in solution is consistent with our interpretation that the drop in pH at the membrane surface plays a role in the mechanism of lipid-induced protein unfolding. However, it is unclear whether the interaction with lipid also accelerates the Met 80 deligation step. Second, the observed rate of 1.5 s^{-1}, despite being measured at a higher temperature (20 °C), is slower than the deligation-limited unfolding rate in solution at pH 7.0 (50 s^{-1}; 10 °C). This further confirms our assignment of the main kinetic phase observed in lipid-induced unfolding (monitored either by fluorescence or by Soret absorbance) to the main structural unfolding event. Finally, the comparison of the rate of lipid-induced unfolding with that extrapolated to zero denaturant concentration (5×10^{-6} s^{-1} at pH 7) clearly indicates that the overall unfolding of cytochrome *c* is substantially accelerated by the interaction with the lipid membrane.

Kinetic Mechanism of Cytochrome c Interaction with Lipid Membranes. Combining our fluorescence-detected kinetic results with those for lipid- and acid-induced unfolding of cytochrome *c* monitored by Soret absorbance, together with the well-characterized folding mechanism of cytochrome *c* in solution, we propose the kinetic mechanism shown in Figure 8. In this scheme, species in *water* are labeled with the superscript *W*, intermediate states on the *surface* of the lipid vesicle have the superscript *S*, and a superscript *L* indicates a *lipid* phase inserted specie. *Native*, fully folded, states are represented by N; M symbolizes destabilized native-like states lacking Met 80 iron ligation [represented by N* in Colón *et al.* (1996), and by M in Sauder *et al.* (1996)]; and I states are associated with compact kinetic intermediates. In our kinetic mechanism, states N and M appear both in water and in association with the membrane surface (N^S and M^S are the surface-associated analogues of N^W and M^W, respectively). The methionine-deligated state (M) is likely to occur also in lipid-induced unfolding (M^S), because M^W is a well-established obligatory unfolding intermediate in water (Colón *et al.*, 1996; Sauder *et al.*, 1996). I^W is a well-characterized compact intermediate that accumulates within milliseconds of refolding in solution, both under native conditions (Elöve *et al.*, 1992, 1994; Sosnick *et al.*, 1996) and in the formation of the A-state at pH 2 (Colón & Roder, 1996). The *unfolded* state in water is represented by U^W, and the *denatured* state inserted in the lipid membrane is designated by D^L. Based on our equilibrium spectroscopic data, D^L has native-like helical secondary structure (Figure 3), but is at least partially unfolded in terms of (a) Trp 59 fluorescence (Figure 2), which shows that the average Trp 59−heme distance is much larger than in the native state, (b) lack of specific native interactions involving Trp 59 (absence of sharp bands at 282 and 288 nm in Figure 4), (c) perturbed heme ligation and heme environment, revealed by the absence of the 695 nm band (Figure 1), and the changes in near-UV and Soret regions of CD spectra (Figures 4 and 5). D^L is clearly a more unfolded state than the equilibrium acid-denatured A-state, but it is not equivalent to the fully unfolded state in water, U^W. While in solution this state is extensively unfolded without stable secondary structure, the lipid-inserted denatured state, D^L, is extensively folded at the secondary structure level (Figure 3). In this sense, D^L may be structurally more closely related to I^W than to U^W.

The comparison between the observed unfolding rate for cytochrome *c* upon binding to DOPS vesicles (~1.5 s^{-1}) with that in solution [about 2×10^{-3} s^{-1} at pH 5.0; unpublished;

see also Sosnick *et al.* (1996)] indicates that lipid-induced unfolding follows a predominant pathway through N^S and M^S (Figure 8). Our observations are consistent with the following scenario. The interaction of native folded cytochrome *c* (N^W) with anionic lipid membranes, such as DOPS vesicles, is initially driven by the electrostatic attraction between positively charged residues in the protein and the negatively charged lipid headgroups in the membrane surface. This first binding step (formation of N^S) is probably diffusion-controlled and occurs during the dead time of the stopped-flow experiments (<2 ms). After binding to the lipid surface, cytochrome *c* is exposed to a locally acidic environment, which is known to induce protein unfolding in bulk aqueous solution [for a review, see Ptitsyn (1995)]. In parallel with the unfolding mechanism of cytochrome *c* in solution (Colón *et al.*, 1996), we expect that the unfolding reaction starts with disruption of Met 80 (formation of M^S). This destabilized conformation unfolds at a rate of $\sim$1.5 s^{-1}. Thus, the rate-limiting step in the observed lipid-induced unfolding event (by fluorescence- or absorbance-detected kinetics) represents the transition of M^S to D^L; *i.e.*, the disruption of the core that makes hydrophobic residues (*e.g.*, in amphipathic helices) available for interaction with the lipid phase ($\sim$1.5 s^{-1}).

In conclusion, we have observed that binding of cytochrome *c* to negatively charged lipid membranes induces unfolding of the native structure of cytochrome *c*. In the presence of lipid vesicles, the rate of unfolding is dramatically accelerated relative to the free protein in solution. Our results are consistent with a mechanism for lipid-induced unfolding triggered by the local decrease in effective pH at the membrane surface. Our findings raise some interesting questions with respect to protein folding in general, and protein folding in membrane environments in particular. For instance, the membrane-bound intermediate, D^L, might represent a stable analogue of a kinetic intermediate in solution trapped in the lipid phase (stabilized by favorable hydrophobic interactions with the lipid membrane), which may escape detection in solution folding studies. The proposed formation of a perturbed compact state (M^S) prior to membrane insertion has implications with respect to protein insertion and translocation into membranes. Compact intermediates (molten globule-like states) have been postulated to be involved in the mechanism of protein insertion and translocation across lipid membranes (Bychkova *et al.*, 1988; Van der Goot, 1992; Banuelos & Muga, 1995). This appears to be the case for the interaction of cytochrome *c* with negatively charged lipid membranes, and may well represent a general mechanism for activation of protein insertion and translocation in the cell.

ACKNOWLEDGMENT

We thank the Oxford Centre for Molecular Sciences for the use of the CD facility. We are grateful to Drs. S. Khorasanizadeh and A. K. Bhuyan for some helpful experimental assistance during T.J.T.P. visits to Fox Chase, and to Dr. W. Colón for critical reading of the manuscript.

REFERENCES

Babul, J., & Stellwagen, E. (1971) *Biopolymers 10*, 2359−2361.
Babul, J., & Stellwagen, E. (1972) *Biochemistry 11*, 1195−1200.
Banuelos, S., & Muga, A. (1995) *J. Biol. Chem. 270*, 29910−29915.
Banuelos, S., & Muga, A. (1996) *Biochemistry 35*, 3892−3898.
Brems, D. N., & Stellwagen, E. (1983) *J. Biol. Chem. 258*, 3655−3660.
Bushnell, G. W., Louie, G. V., & Brayer, G. D. (1990) *J. Mol. Biol. 214*, 585−595.
Bychkova, V. E., & Ptitsyn, O. B. (1993) *Chemtracts*: *Biochem. Mol. Biol. 4*, 133−163.
Bychkova, V. E., Pain, R. H., & Ptitsyn, O. B. (1988) *FEBS Lett. 359*, 6−8.
Chang, C. T., Wu, C.-S. C., & Yang, J. T. (1978) *Anal. Biochem. 91*, 13−31.
Colón, W., & Roder, H. (1996) *Nat. Struct. Biol. 3*, 1019−1025.
Colón, W., Elöve, G. A., Wakem, L. P., Sherman, F., & Roder, H. (1996) *Biochemistry 35*, 5538−5549.
Cowan, S. W., Newcomer, M. E., & Jones, T. A. (1990) *Proteins: Struct., Funct., Genet. 8*, 44−61.
Davies, A. M., Guillemette, J. G., Smith, M., Greenwood, C., Thurgood, A. G. P., Mauk, A. G., & Moore, G. R. (1993) *Biochemistry 32*, 5431−5435.
De Jongh, H. H. J., Killian, J. A., & de Kruijff, B. (1992) *Biochemistry 31*, 1636−1643.
Dyson, H. J., & Beattie, J. K. (1982) *J. Biol. Chem. 257*, 2267−2273.
Elöve, G. A., Chaffotte, A. F., Roder, H., & Goldberg, M. E. (1992) *Biochemistry 31*, 6876−6883.
Elöve, G. A., Bhuyan, A. K., & Roder, H. (1994) *Biochemistry 33*, 6925−6935.
Evans, P. A., & Radford, S. E. (1992) *Curr. Biol. 4*, 100−106.
Farren, S. B., & Cullis, P. R. (1980) *Biochem. Biophys. Res. Commun. 97*, 182−191.
Gao, Y., Lee, A. D. J., Williams, R. J. P., & Williams, G. (1989) *Eur. J. Biochem. 182*, 57−65.
Ghosh, R. (1988) *Biochemistry 27*, 7750−7758.
Goto, Y., Calciano, L. J., & Fink, A. L. (1990) *Proc. Natl. Acad. Sci. U.S.A. 87*, 573−577.
Gupte, S. S., & Hackenbrock, C. R. (1988a) *J. Biol. Chem. 263*, 5241−5247.
Gupte, S. S., & Hackenbrock, C. R. (1988b) *J. Biol. Chem. 263*, 5248−5253.
Hannavy, K., Rospert, S., & Schatz, G. (1993) *Curr. Opin. Struct. Biol. 5*, 694−700.
Heimburg, T., & Marsh, D. (1993) *Biophys. J. 65*, 2408−2417.
Heimburg, T., Hildebrandt, P., & Marsh, D. (1991) *Biochemistry 30*, 9084−9089.
Hildebrandt, P., & Stockburger, M. (1986) *J. Phys. Chem. 90*, 6017−6024.
Hildebrandt, P., & Stockburger, M. (1989a) *Biochemistry 28*, 6710−6721.
Hildebrandt, P., & Stockburger, M. (1989b) *Biochemistry 28*, 6722−6728.
Hildebrandt, P., Heimburg, T., & Marsh, D. (1990a) *Eur. Biophys. J. 18*, 193−201.
Hildebrandt, P., Heimburg, T., Marsh, D., & Powell, G. L. (1990b) *Biochemistry 29*, 1661−1668.
Hsu, M. C., & Woody, R. W. (1971) *J. Am. Chem. Soc. 93*, 3515−3525.
Jeng, M.-F., Englander, S., Elöve, G. A., Wand, A. J., & Roder, H. (1990) *Biochemistry 29*, 10433−10437.
Kimbelberg, H. K., & Lee, C. P. (1970) *J. Membr. Biol. 2*, 252−262.
Koppenol, W. H., & Margoliash, E. (1982) *J. Biol. Chem. 257*, 4426−4437.
Lakey, J. H., Gonzalez-Manas, J. M.,Van der Goot, F. G., & Pattus, F. (1992) *FEBS Lett. 307*, 26−29.
Margoliash, E., & Schejter, A. (1966) *Adv. Protein Chem. 21*, 113−286.
Margoliash, E., & Walasek, O. F. (1967) *Methods Enzymol. 10*, 339−348.
Muga, A., Mantsch, H. H., & Surewicz, W. K. (1991a) *Biochemistry 30*, 2629−2635.
Muga, A., Mantsch, H. H., & Surewicz, W. K. (1991b) *Biochemistry 30*, 7219−7224.
Myer, Y. P. (1968a) *Biochemistry 7*, 765−776.
Myer, Y. P. (1968b) *J. Biol. Chem. 243*, 2115−2122.
Parker, M. W., & Pattus, F. (1993) *Trends Biochem. Sci. 18*, 391−395.

Pinheiro, T. J. T. (1994) *Biochimie 76*, 489−500.
Pinheiro, T. J. T., & Watts, A. (1994a) *Biochemistry 33*, 2451−2458.
Pinheiro, T. J. T., & Watts, A. (1994b) *Biochemistry 33*, 2459−2467.
Prats, M., Teissié, J., & Toccane J. F. (1986) *Nature 322*, 756−758.
Pryse, K. M., Bruckman, T. G., Maxfield, B. W., & Elson, E. L. (1992) *Biochemistry 31*, 5127−5136.
Ptitsyn, O. B. (1995) *Adv. Protein Chem. 47*, 83−229.
Radford, S. E., Dobson, C. M., & Evans, P. A. (1992) *Nature 358*, 302−307.
Ramdas, L., & Nall, B. T. (1986) *Biochemistry 25*, 6959−6964.
Roder, H., Wand, A. J., Milne, J. S., & Englander, S. W. (1986) *Biophys. J. 49*, 57a.
Roder, H., Elöve, G. A., & Englander, S. W. (1988) *Nature 335*, 700−704.
Santucci, R., Giartosio, A., & Ascoli, F. (1987) *Biochim. Biophys. Acta 914*, 185−189.
Santucci, R., Giartosio, A., & Ascoli, F. (1989) *Arch. Biochem. Biophys. 275*, 496−504.
Sauder, J. M., MacKenzie, N. E., & Roder, H. (1996) *Biochemistry 35*, 16852−16862.
Sosnick, T. R., Mayne, L., & Englander, S. W. (1996) *Proteins: Struct., Funct., Genet. 24*, 413−426.
Spooner, P. J. R., & Watts, A. (1991a) *Biochemistry 30*, 3871−3879.
Spooner, P. J. R., & Watts, A. (1991b) *Biochemistry 30*, 3880−3885.
Spooner, P. J. R., & Watts, A. (1992) *Biochemistry 31*, 10129−10138.
Spooner, P. J. R., Duralski, A. A., Rankin, S. E., Pinheiro, T. J. T., & Watts, A. (1993) *Biophys. J. 65*, 106−112.
Stellwagen, E., & Babul, J. (1975) *Biochemistry 14*, 5135−5140.
Strickland, E. H. (1974) *CRC Crit. Rev. Biochem. 2*, 113−175.
Tsong, T. Y. (1975) *Biochemistry 14*, 1542−1547.
Urry, D. W. (1967) *J. Biol. Chem. 242*, 4441−4448.
Van der Goot, F. G., Gonzalez-Manas, J. M., Lakey, J. H., & Pattus, F. (1991) *Nature 354*, 408−410.
Van der Goot, F. G., Lakey, J. H., & Pattus, F. (1992) *Trends Cell Biol. 2*, 343−348.
Vik, S. B., Georgevich, G., & Capaldi, R. A. (1981) *Proc. Natl. Acad. Sci. U.S.A. 78*, 1456−1460.

BI971235Z